

Section: Earth science

### **Reservoir Characterization of Upper Bahariya formation (Cenomanian) in North Qarun oil Field, Western Desert, Egypt.**

Ahmed Soliman Ahmed

Tharwat Helmy Abdel Hafeez

Mohamed Mosaad Mohamed

# Reservoir Characterization of the Upper Bahariya Formation (Cenomanian) in the North Qarun Oil Field, Western Desert, Egypt

Ahmed Soliman Ahmed <sup>a,\*</sup>, Tharwat Helmy Abdel Hafeez <sup>b</sup>, Mohamed Mosaad Mohamed <sup>b</sup>

<sup>a</sup> Khalda Petroleum Company, Cairo, Egypt

<sup>b</sup> Department of Geology, Faculty of Science, Al-Azhar University, Cairo, Egypt

## Abstract

Our aim is to understand the subsurface system and the characteristics of the Upper Bahariya reservoir within the North Qarun oil field, spanning from well to multi-well and field scales. The current study focuses on integrating a wide spectrum of datasets to achieve a comprehensive and coherent characterization of the Upper Bahariya Formation. This endeavor is essential for formulating an effective field development plan (FDP) and enhancing oil recovery efforts. The study entails the integration and interpretation of well-logging analyses and 3-D seismic data from four wells strategically distributed across the North Qarun oil field. A detailed structural interpretation is conducted to determine the structural geometry of the horizons. Petrophysical analyses are performed on the Upper Bahariya reservoir, with petrophysical properties mapped to illustrate lateral variations in the study area. These variations are crucial for predicting reservoir geometry and devising suitable development plans for new wells.

**Keywords:** Egypt, North Qarun, Reservoir characterization, Well-logging analysis, Western Desert

## 1. Introduction

The North Qarun oil field, our study area, is situated within the Qarun Concession. It lies on the southeastern flank of the Kattaniya inverted basin and the northwestern flank of the Gindi basin, positioned between latitudes 29°47'.8233' and 29°48'.9404' N and longitudes 30°36'.1373' and 30°32'.2964' E, covering approximately 8.5 km<sup>2</sup> (Fig. 1). The presence of hydrocarbons in this area is intricately tied to tectonic activities and the stratigraphic history, which have created a series of reservoirs and seals. Many fields in the north Western Desert owe their existence to structures formed during the Late Cretaceous–Eocene period, situated within or at the periphery of early depocenters that eventually transformed into kitchen areas [1]. The thick Khatatba mixed prone source

rock has produced significant amounts of oil, which migrated southward and eastward to charge the North Qarun field during and after basin inversion. The Qarun Concession serves as a prime example of these structural activities, with numerous discovery wells drilled by various operators. For instance, the El-Sagha – IX (Qarun – I) well identified hydrocarbon potential in the Kharita and Lower Bahariya Formations but was lost due to mechanical issues. The El-Sagha-3X (Qarun 3) appraisal well, drilled updip from the first well, encountered more than 300 feet of net oil pay in the Bahariya and Kharita sandstones, producing at a rate of ±12,000 BOPD of 42° API from both reservoirs. However, unplanned drilling activities in the 1990s resulted in several dry holes in the highly inverted Kattaniya Basin, attributed to issues with hydrocarbon charging and/or sealing problems [2].

Received 18 March 2024; revised 24 July 2024; accepted 28 July 2024.  
Available online 18 October 2024

\* Corresponding author at: Khalda Petroleum Company, Road 290, 560-Maadi, New Maadi, Cairo, Egypt.  
E-mail address: [ahmedsolomahmed87@gmail.com](mailto:ahmedsolomahmed87@gmail.com) (A.S. Ahmed).

<https://doi.org/10.58675/2636-3305.1683>

2636-3305/© 2024, The Authors. Published by Al-Azhar university, Faculty of science. This is an open access article under the CC BY-NC-ND 4.0 Licence (<https://creativecommons.org/licenses/by-nc-nd/4.0/>).

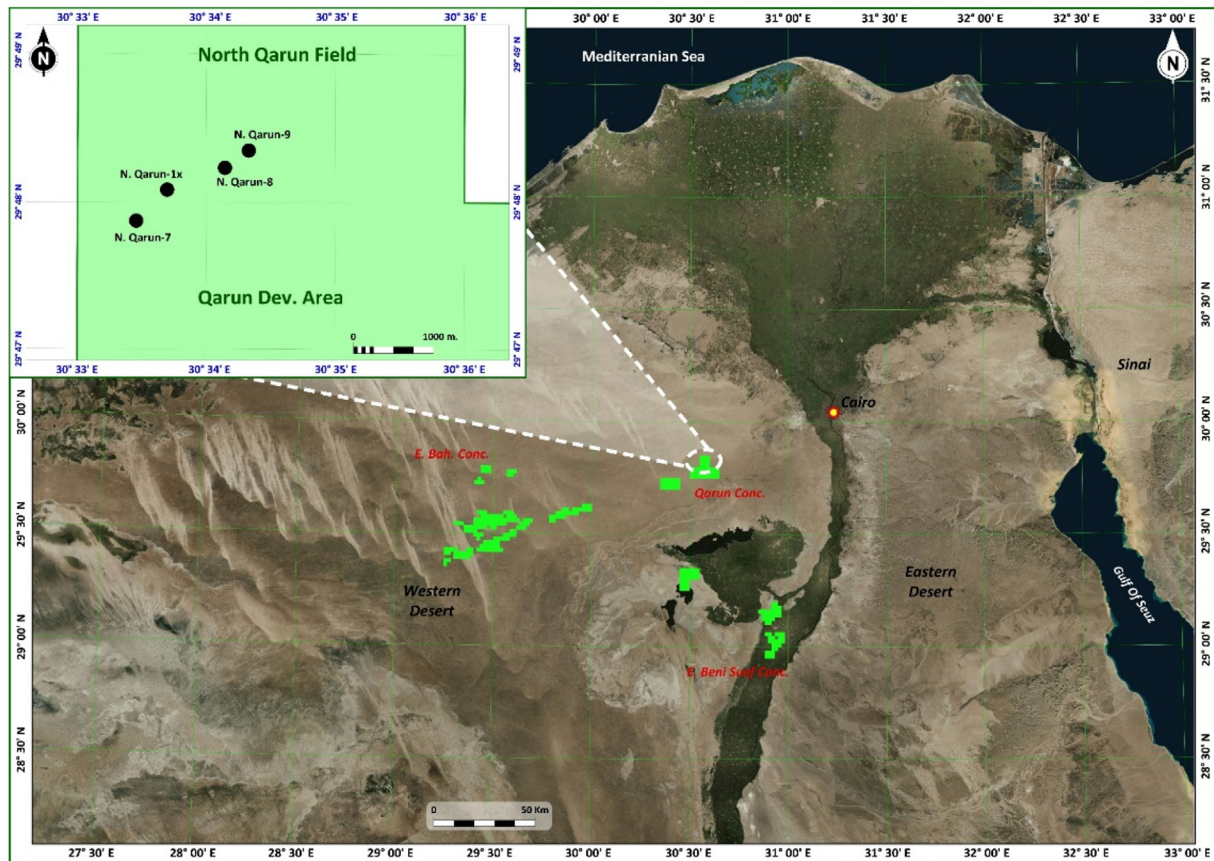


Fig. 1. Location map shows the study area with reference to Egypt.

## 2. Geological setting

### 2.1. Stratigraphy

The geological setup of the North Western Desert reveals a substantial stratigraphic section characterized by diverse strata, ranging in thickness from approximately 100 feet (as exemplified by Abu Roash F Mbr.) to 3000 feet (as observed in Kharita Fm.). These sediments display varied facies including shale, siltstone, limestone, and sandstone which gradually increases in thickness toward the northeast, reaching an estimated 7620 m [3]. The sedimentary sequence within the study area, as inferred from the deepest drilled well, spans from the Precambrian Basement relief to the Miocene Moghra Formation at the surface. Within the Qarun Concession located in the Gindi Basin, the stratigraphy can be delineated into three distinct provinces: the Kattaniya province to the northwest of Birket Qarun, the El-Sagha province at the northern boundaries of Birket Qarun, and the Wadi El-Rayan province to the south of Birket Qarun [4]. The Upper Cretaceous section, inclusive of the

Upper Bahariya reservoir, is noted for its deposition in a tidal flat environment with agitated currents, leading to alternating intercalations between sandstone and siltstone, interspersed with shale and carbonate laminae, resulting in heterogeneity both vertically and laterally. The accompanying figure illustrates the stratigraphic column in the Qarun Concession juxtaposed with the generalized stratigraphic column for the North Western Desert (Fig. 2) [5].

### 2.2. Tectonic and structural perspective

The structural evolution of the North Western Desert from the Late Jurassic to Early Tertiary periods seems to have been significantly influenced by two primary tectonic forces associated with Tethyan plate movements. First, sinistral shear, occurring during the Late Jurassic to Early Cretaceous period, and second, dextral shear, prevailing during the Late Cretaceous to the Paleocene era [6,7].

The Northern Western Desert experienced three major tectonic events: (a) Jurassic and Early

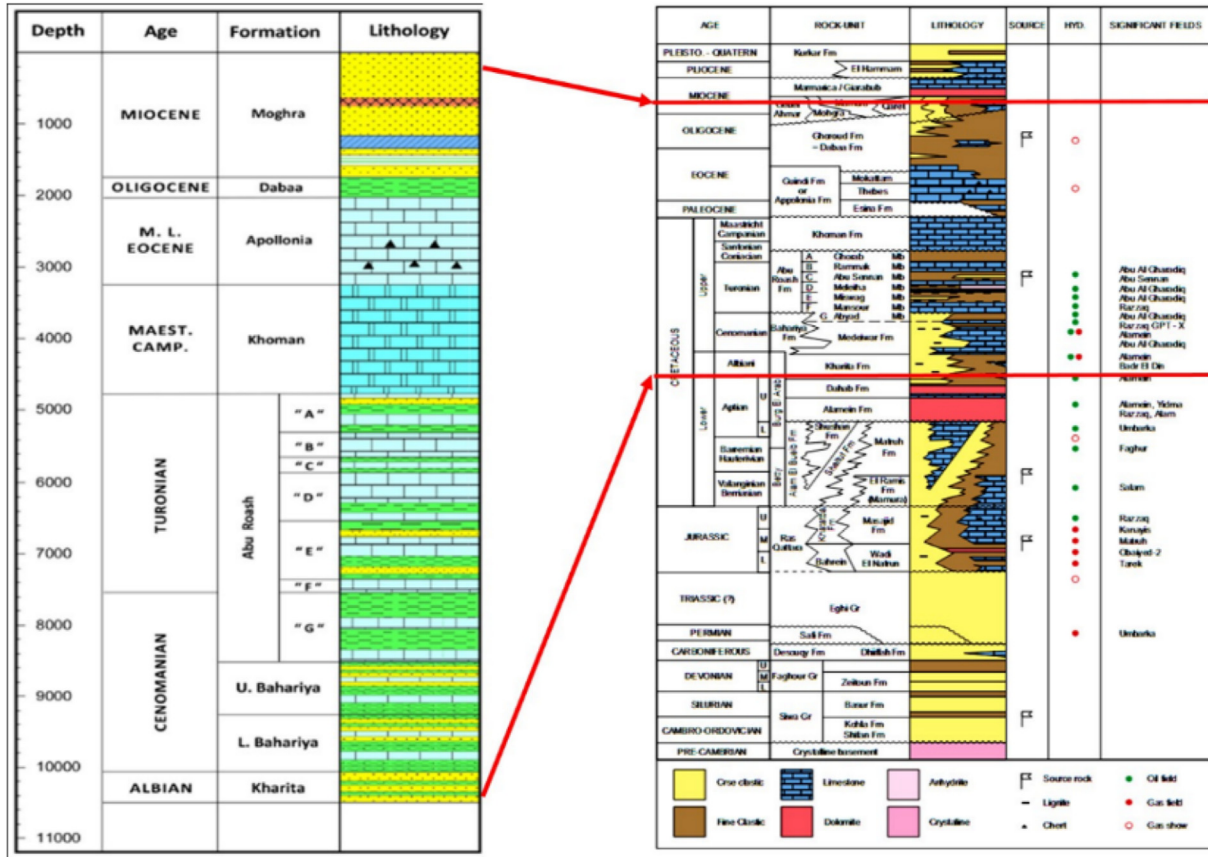


Fig. 2. Generalized stratigraphic column of north Western Desert shows the lithological cyclicality.

Cretaceous rifting. (b) Late Cretaceous–early tertiary positive structural inversion. (c) Miocene and post-Miocene extension.

These tectonic activities resulted in the formation of basins, including N and NE-tilted half grabens during the Jurassic and Early Cretaceous, responding to the opening of the NeoTethys and Atlantic oceans, respectively. The Qarun Concession lies within the Kattaniya inverted basin, oriented NE-SW and situated in the easternmost part of the North Western Desert (Fig. 3) [8].

This basin underwent an early rifting phase during the Jurassic and Cretaceous periods, leading to the accumulation of northward thickening rock layers against a major NE-SW-oriented fault with southeast-directed throw [9].

Subsequently, the basin experienced inversion during the Late Cretaceous–early tertiary period, resulting in the development of several NE-SW-oriented anticlines bounded by reverse faults. The significant uplift during basin inversion led to erosion of Upper Cretaceous rocks in highly inverted zones, while deeply buried anticlines to the south

remained intact and capable of trapping hydrocarbons, such as in the Qarun, North Qarun, Southwest Qarun, WD-19, and Wadi El-Rayan fields [10].

The North Qarun oil field is characterized by structurally controlled traps, represented as an echelon structures of NE double plunging anticlines bounded by NE reverse faults and dissected by NW normal faults, which were reactivated during the opening of the Gulf of Suez.

### 3. Materials and methods

Materials and methods used in this study primarily involved the interpretation of two-dimensional seismic lines exported from three-dimensional (3D) seismic cube, encompassing 10 X-lines, eight in-lines, and two arbitrary lines. Moreover, well log analysis was conducted, using various logs including SP, GR, resistivity, and density, neutron, and calliper logs from four wells (NQ-1, NQ-7, NQ-8, NQ-9) in the North Qarun oil field. The seismic interpretation was carried out by picking fault interpretation and stratigraphic horizons (Apollonia, Khoman, Abu

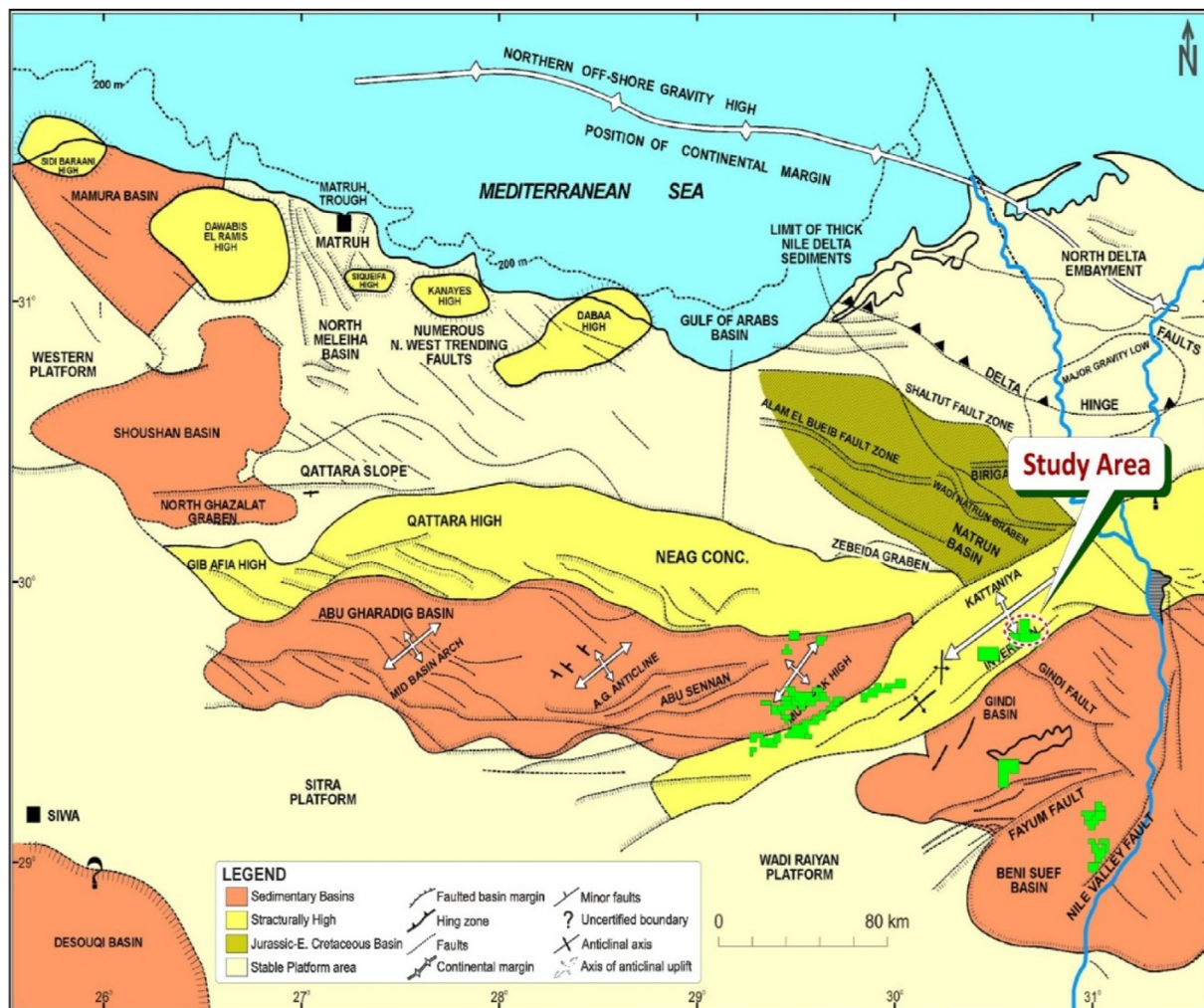


Fig. 3. Tectonic framework in the Western Desert of Egypt (modified after Bayoumi 1996).

Roash “G,” Abu Roash “D,” Abu Roash “C,” and Abu Roash “A” members, Lower and Upper Bahariya and Kharita). Both stratigraphic horizons and fault interpretation resulted from the seismic data of the interesting section used in construction 3D structural model using Petrel software, resulting in the generation of structure maps for the target reservoirs. The well log analysis was performed using Interactive Petrophysics software, facilitating computer-processed interpretation for the drilled wells. Determine the petrophysical characteristics such as net pay, effective porosity, shale content, water saturation, and hydrocarbon saturation to assess Bahariya reservoir potentiality. Moreover, mapping of net pay and sand distribution among the wells was conducted, alongside the creation of average water saturation, average effective porosity, and average shale content maps.

The integration of available subsurface geological and geophysical data is essential to study the

reservoir characterization and processes that control hydrocarbon potentialities of the study area with special emphasis on the Cretaceous sequence.

## 4. Results and discussion

### 4.1. Southwest Northeast trending seismic section (arbitrary line)

The chosen seismic section (arbitrary line) was analyzed to demonstrate horizon picking and structural features within the study area. This section showcases nine seismic reflectors that were identified, including formations such as the Kharita Formation, Lower and Upper Bahariya, Abu Roash “G,” Abu Roash “D,” Abu Roash “C,” and Abu Roash “A” members, as well as the Khoman and Apollonia (Fig. 4). The North Qarun oil field forms part of a structural complex measuring 15 km NE-

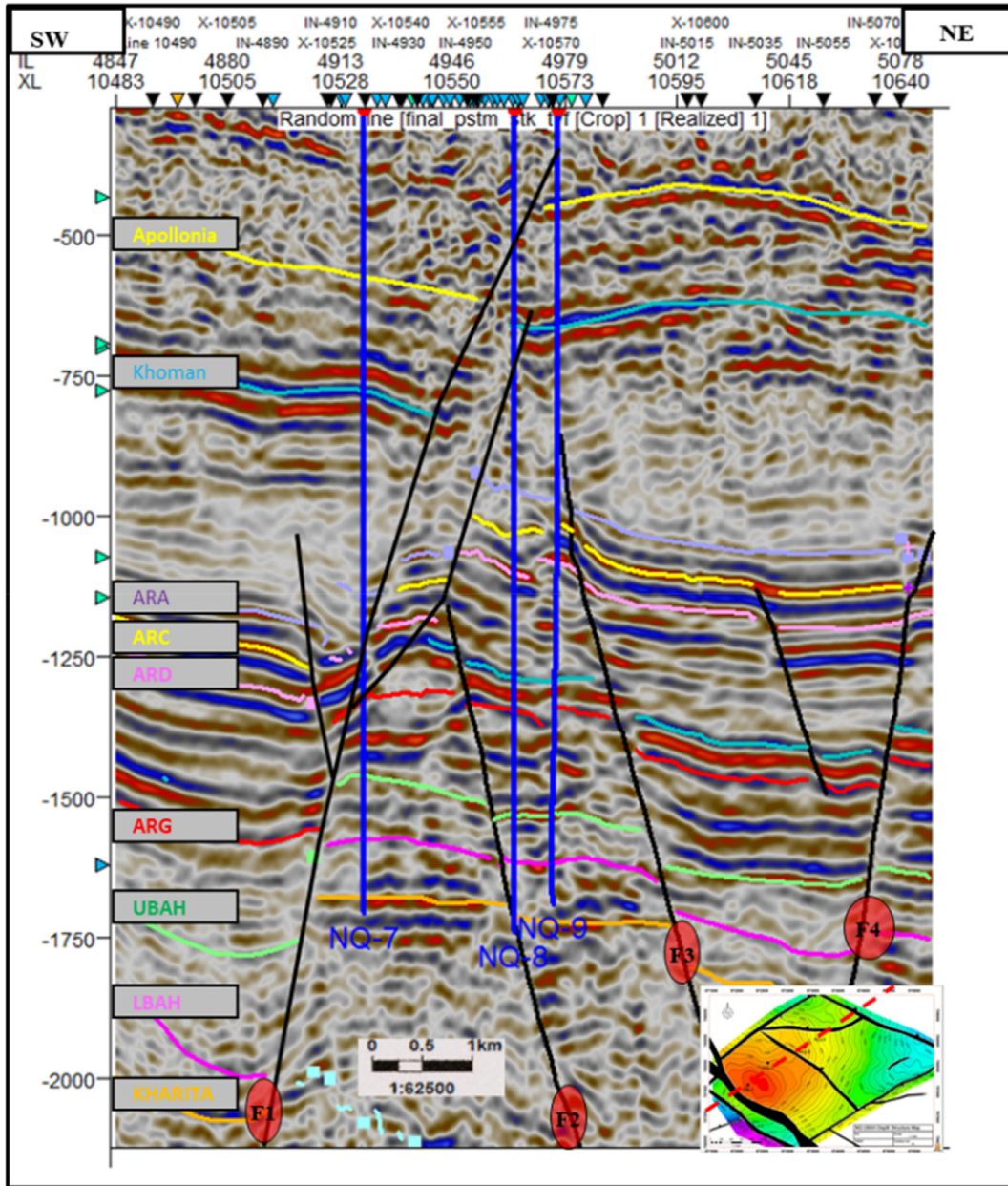


Fig. 4. SW–NE seismic section (arbitrary line) passing through NQ-7, NQ-8, and NQ-9 illustrates the structure setting.

SW and 5 km NW-SE, aligning with the regional study.

The section exhibits NE-SW trending normal faults (F1, F2, and F4) and one E-W trending normal fault (F3). Primary normal fault in the North Qarun field, (F1) trends in a Northwest-Southeast direction, intersecting members from the A/R “A” Member to the Kharita Formation. This fault formation creates effective traps on the up thrown side. Moreover, F2 intersects members from the A/R “D” Member to below the Kharita Formation, while F3 cuts across members from

the A/R “A” member to below the Kharita Formation. The Upper Bahariya Formation is observed as a sliver faulted block bounded by F2 and F3. Furthermore, F4 intersects members from the A/R “A” member to below the Kharita Formation.

#### 4.2. Depth structure contour map

The depth structure contour map delineating the top of the Upper Bahariya, derived from 3D seismic data in the NQ Field area, is illustrated (Fig. 5). It

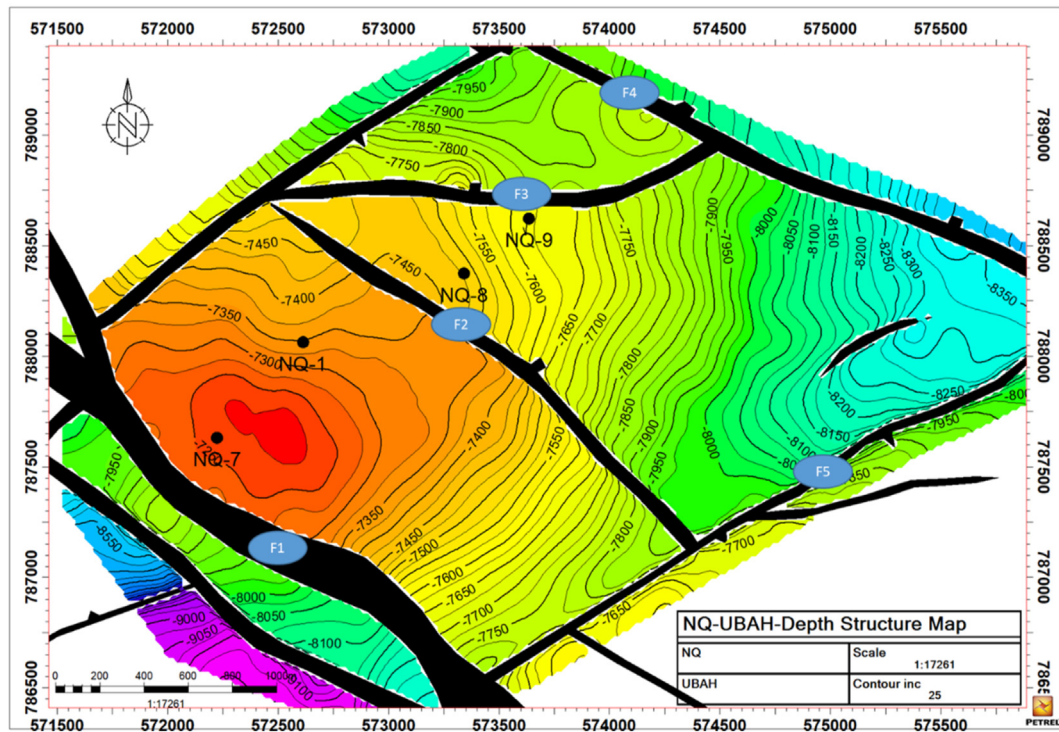


Fig. 5. Depth structure map of the top Upper Bahariya shows different faults affecting the reservoir geometry.

reveals an echelon structures characterized by NE double plunging anticlines bordered by NE reverse faults and intersected by NW normal faults.

The study area exhibits a structurally positive inverted configuration, bounded by two prominent reverse faults. The southeastern and northwestern sections of the study area, situated in low-structure regions, register depths ranging between 7800 and 8300 feet on both sides. Conversely, the central high-structure portion of the study area records depths around 7225 feet.

#### 4.3. Well-logging analysis

Interpreting well logs entails selecting the most suitable model from the available data to derive accurate results. This involves integrating all geological insights obtained from the thorough analysis of logs, encompassing parameters such as porosity, water saturation, permeability, and their respective sums and averages. Particularly, the interpretation of water saturation (SW) necessitates the integration of true formation resistivity (RT) and porosity ( $\emptyset$ ).

##### 4.3.1. Neutron-density cross-plot

Neutron-density cross plots are widely used for lithology determination and precise matrix porosity

assessment in carbonate formations, leveraging neutron and density logs. This method involves plotting bulk density (RHOB) against neutron porosity (NPHI) [11]. Through this integrated approach, diverse lithological components such as sandstone, siltstone, shale, and limestone can be identified. To delineate the reservoir effectively, the Upper Bahariya can be subdivided into 10 zones, with particular focus on two significant zones (UB-1, UB-2).

Figure 6 shows the neutron-density cross-plot applied to the UB-1 zone across multiple wells (NQ-1, NQ-7, NQ-8, and NQ-9) are depicted. The UB-1 zone exhibits a range from clean sand grading to silty facies. Notably, the NQ-1 well exhibits the most favorable reservoir properties, with an average effective porosity of 20%, whereas the NQ-9 well showcases lower-quality reservoir facies.

Figure 7 shows a cross-plot illustrating the neutron-density relationship through UB-2 zone across multiple wells (NQ-1, NQ-7, NQ-8, and NQ-9). Similar to UB-1, the UB-2 zone encompasses a range from clean sand grading to silty facies. Here, the NQ-7 well stands out with the best reservoir properties, boasting an average porosity of 17%, while the NQ-8 well exhibits lower-quality reservoir facies.

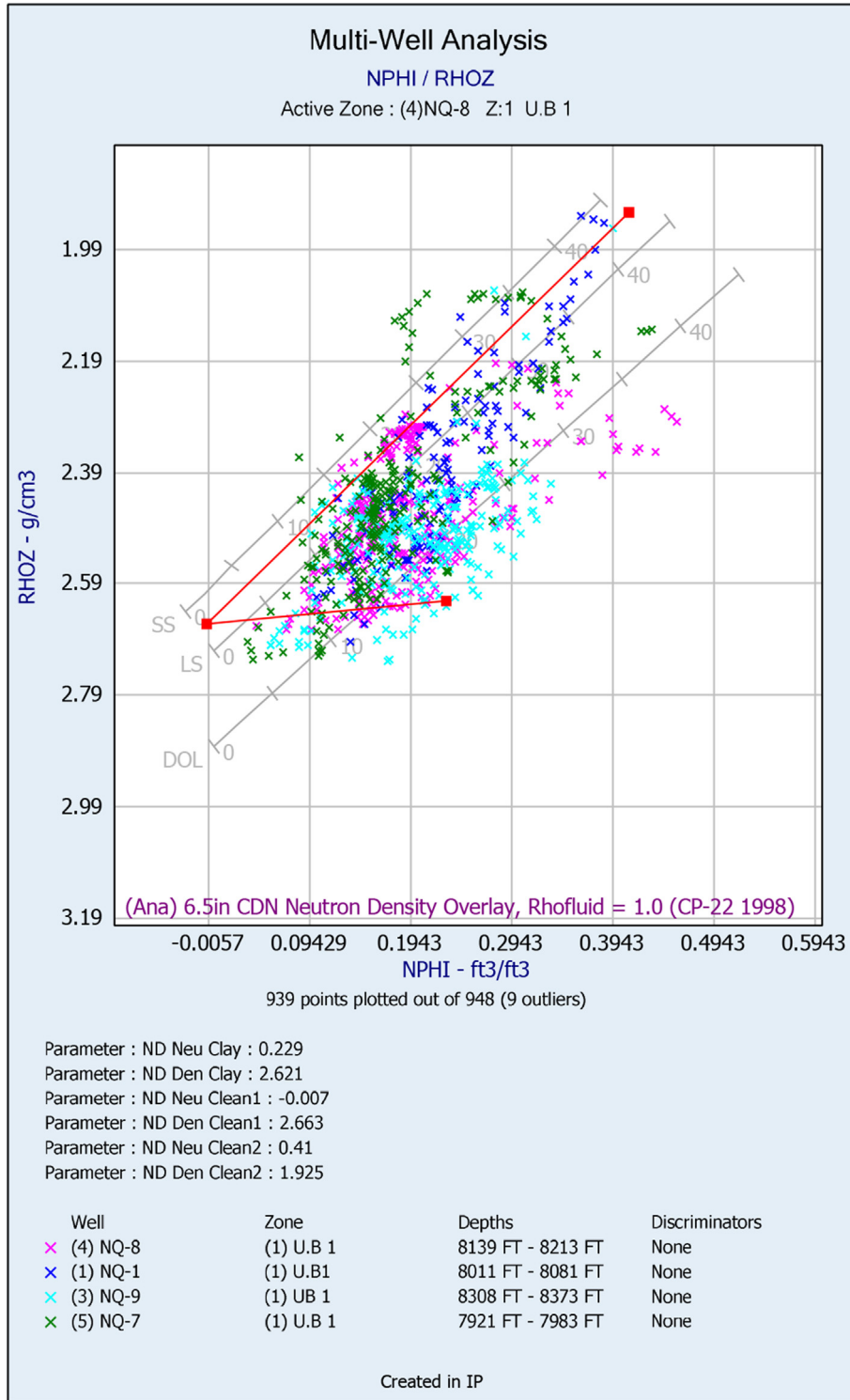


Fig. 6. Neutron-density cross-plot of the UB-1 zone shows range from clean sand grading to silty facies.



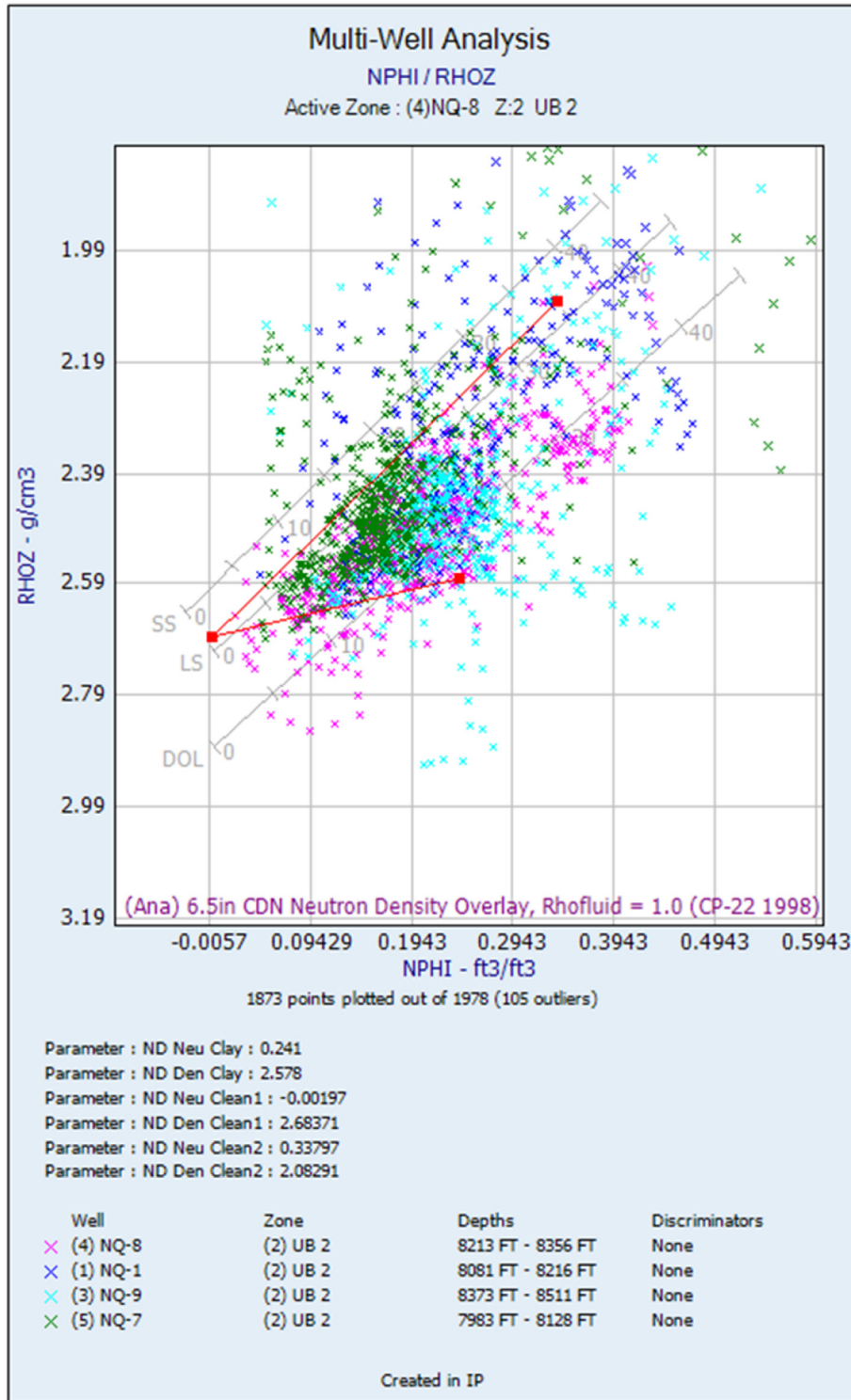


Fig. 7. Neutron-density cross-plot of the UB-2 zone among all wells in the study area.

4.3.2. Determination of formation water resistivity

Water resistivity ( $R_w$ ) was acquired for Bahariya Formation by using a Pickett plot. Pickett plot is the relation between porosity and resistivity. The Pickett plot is a visual representation of the Archie equation and therefore is a powerful graphic technique for estimating SW ranges within a reservoir.

Figure 8 shows a Pickett plot illustrating the porosity–resistivity relationship through the Bahariya Formation (NQ-8 well). Cross plotted points that lie above the water line have water saturations of less than 100% and complementary hydrocarbon saturations. The line has a slope of  $m$ , which is determined manually by measuring a distance on the  $R_t$  axis and dividing it by the corresponding distance on the porosity axis. The intercept when  $PHI = 1$  is the value of an  $R_w$ , and by knowing the value of  $R_w$ , the value of tortuosity factor ( $a$ ) can be

determined. The NQ-8 well exhibits ( $m$ ) and ( $a$ ) values as 1.73 and 1, respectively, plus an  $R_w$  value of 0.0914 ohmm at surface temperature and 0.0339 ohmm at formation temperature.

Figures 9 and 10 show Buckles plots for the UB-1 and UB-2 zones through wells NQ-1, NQ-7, NQ-8, and NQ-9, illustrating the relationship between water saturation and effective porosity supported by a set of BVW hyperbola to assess Bahariya reservoir characteristics. In these zones, where BVW values are 0.02 in UB-1 and 0.04 in UB-2, which resulted in the presence of some horizontal  $Sw_{irr}$ . These sections initially produce oil without water in the initial phase. As the BVW values increase, it indicates the production of a mixture of oil and water. Lastly, the highest values shows water production. In the UB-2 zone, most wells show higher water saturation and BVW values,

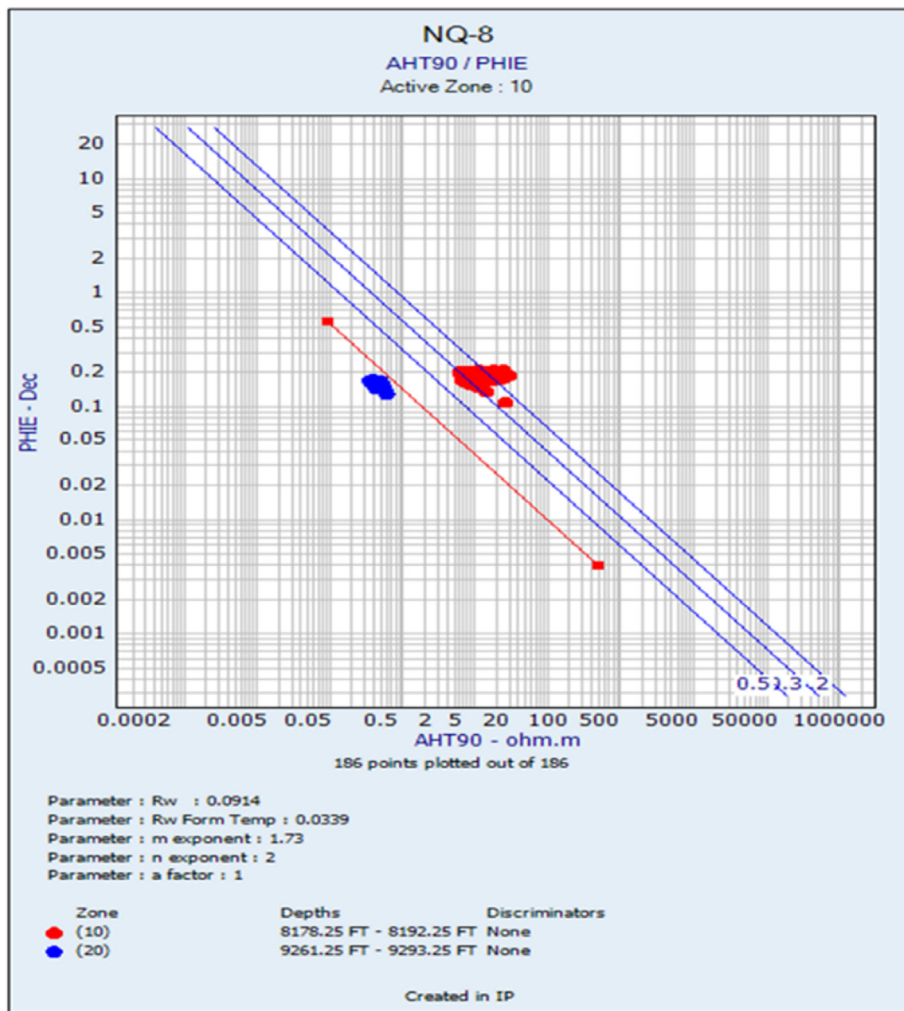


Fig. 8.  $R_w$  Pickett plot of the Bahariya Formation in the NQ-8 well.

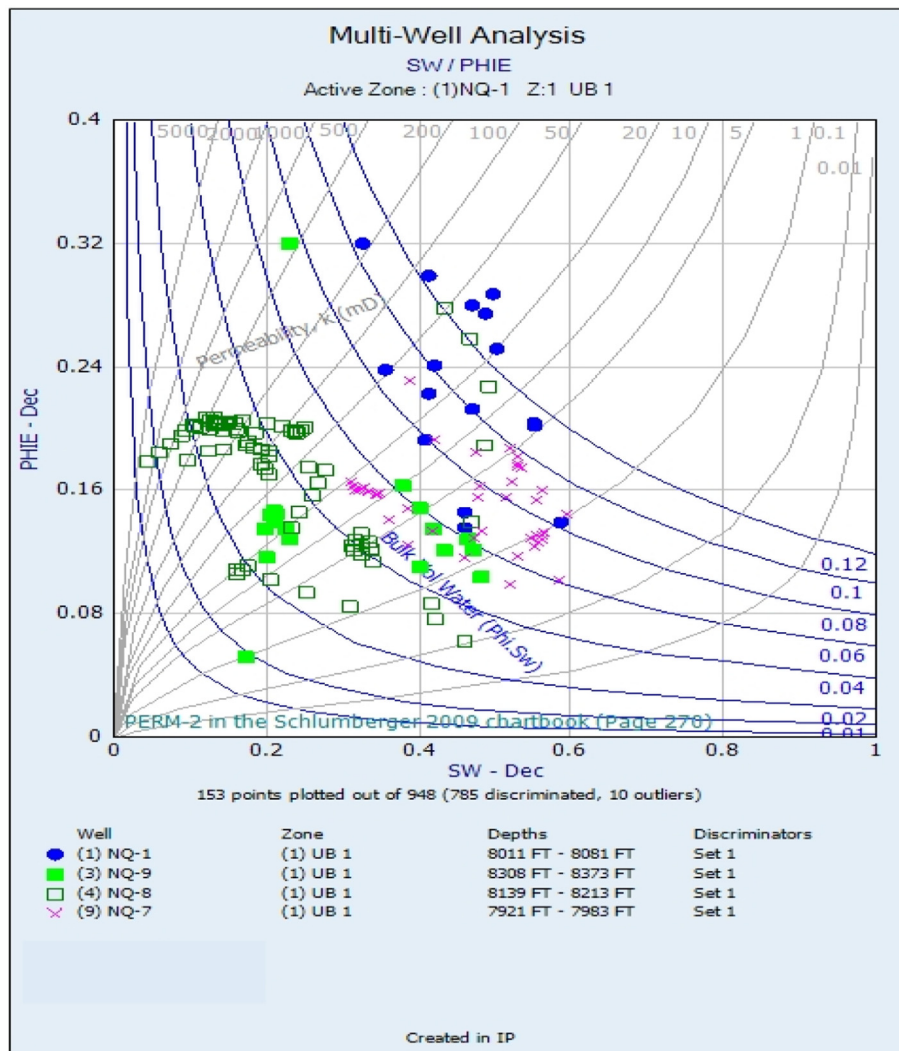


Fig. 9. Buckle plot for the UB-1 zone through NQ-1, NQ-7, NQ-8, and NQ-9 wells.

greater than 0.08, indicating the production of a mixture of oil and water. In the UB-1, all wells show scattered values of water saturation and BVW. NQ-1 and NQ-7 show the highest BVW, indicating a higher proportion of mixed water during the oil production process, which can be due to high porosity values combined with high water saturation. The best well which shows a BVW of less than 0.04 is NQ-8 and NQ-9. These results confirm the low water values in the oil production process.

#### 4.3.3. Cutoffs

Determining cutoffs is essential for distinguishing between intervals with reservoir potential and those without. The key note of using cutoff parameters is to establish the reference range that aid

in reservoir discrimination. The volume of shale cutoff separates sand readings from shale readings, enabling the identification of total sand intervals. These intervals are determined based on relationships between shale volume, sand volume, and effective porosity.

Water saturation cutoff is used to differentiate between productive reservoir intervals (oil sand) and nonpay intervals (wet sand) within porous intervals.

Net pay refers to any interval within the reservoir containing producible hydrocarbons at an economically viable rate. Net pay is crucial for estimating volumetric hydrocarbon reserves and determining reservoir potentiality. Distinguishing between gross and net pay involves applying cutoff values during petrophysical analysis. In the study

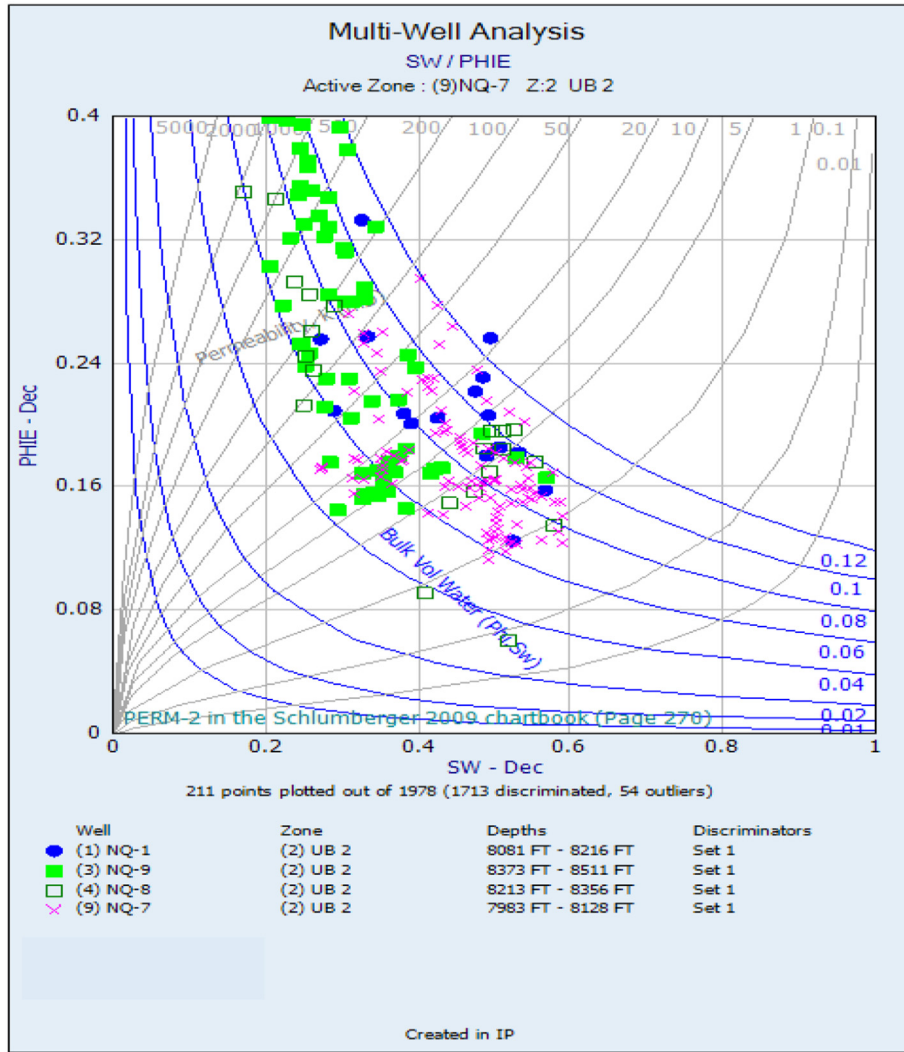


Fig. 10. Buckles plot for the UB-2 zone through NQ-1, NQ-7, NQ-8, and NQ-9 wells.

area, optimal cutoffs were determined from production history, indicating a porosity cutoff of approximately 12%, a clay volume cutoff of less than 30%, and a water saturation cutoff of up to 80%.

4.3.4. Log data analysis results

The interpretation of well logs for all wells in the study area is exemplified by the Upper Bahariya Formation in North Qarun field (Figs. 11–14) and summarized in Tables 1 and 2 as follows.

The first well North Qarun-1 shows 37 ft net pay, with a 22% average effective porosity and 37% average water saturation (Fig. 11).

Regarding the second well, North Qarun-7, it shows nearly same thickness of 36 ft net pay as the first well, featuring an average effective porosity of

16% and an average water saturation of 40% (Fig. 12).

The last two wells North Qarun-8 and North Qarun-9 Wells show 20 and 17 ft net pay, with an average effective porosity of 17 and 16%, accompanied average water saturation for both wells is 35 and 41%, respectively (Figs. 13 and 14).

4.4. Lateral variation of reservoir properties

4.4.1. The net pay distribution

The net pay thickness map for the Upper Bahariya Formation (UB-1, UB-2) in the studied wells of the North Qarun oil field illustrates a trend where the net pay thickness of the Upper Bahariya reservoir (UB-1, UB-2) increases toward the southwest (upstructure), with the NQ-1 well

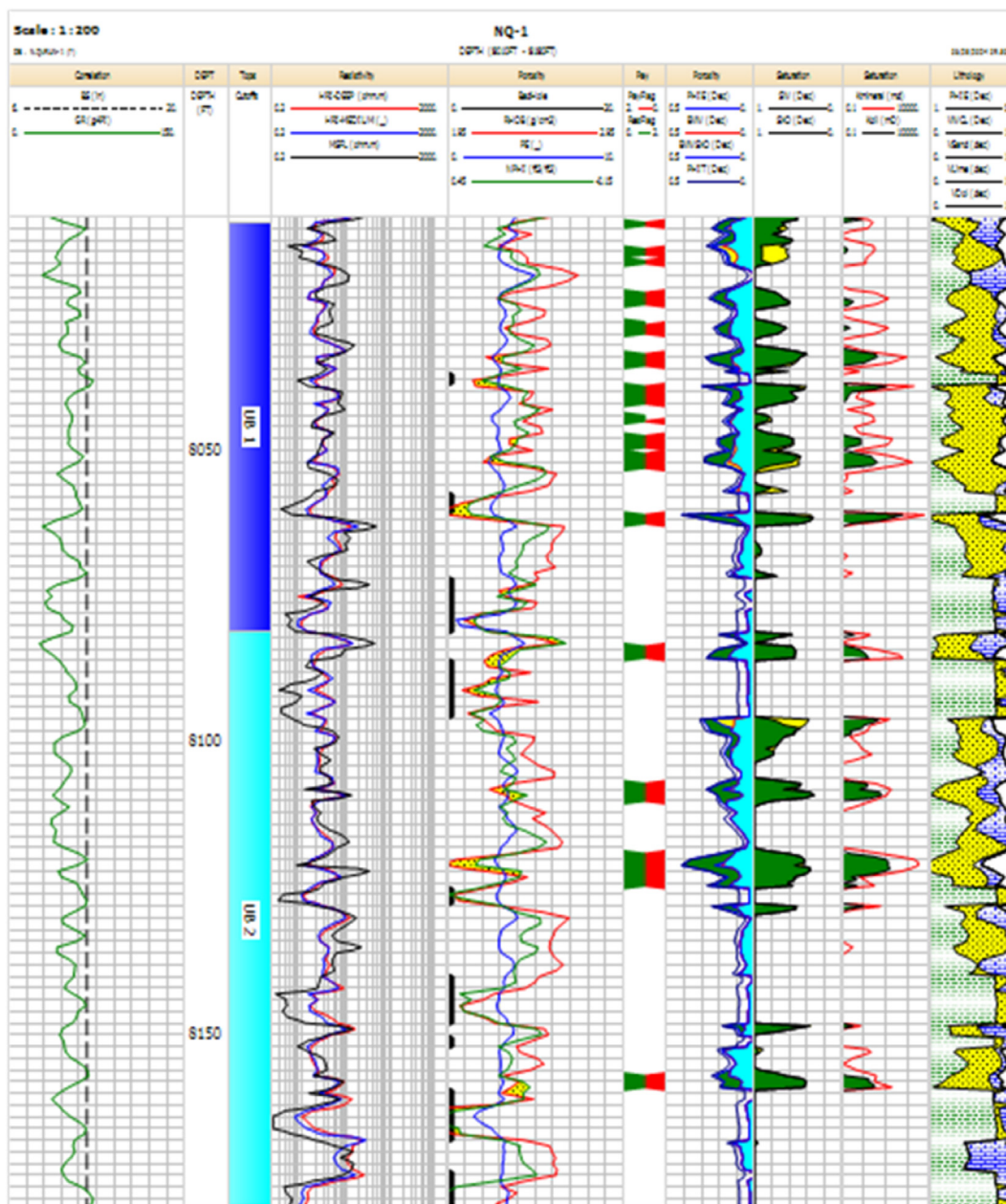


Fig. 11. Petrophysical evaluation for UB-1 and UB-2 zones in the NQ-1 well summarize the pay results and depths.

exhibiting the maximum net pay thickness. Conversely, the net pay thickness decreases toward the northeast (downstructure), with the NQ-9 well showing the minimum net pay thickness. This trend reflects the influence of facies distribution in the field (Fig. 15).

#### 4.4.2. Effective porosity distribution

The effective porosity distribution map for the Upper Bahariya Formation (UB-1, UB-2) in the investigated wells of the North Qarun oil field

shows that effective porosity increases at the central part of the field. The NQ-1 well exhibits the maximum average effective porosity, while NQ-7 and NQ-9 wells show the minimum average effective porosity (Fig. 16).

#### 4.4.3. Volume of clay distribution

The clay volume distribution map for the Upper Bahariya Formation (UB-1, UB-2) in the investigated wells of the North Qarun oil field indicates a decrease in the volume of clay toward the

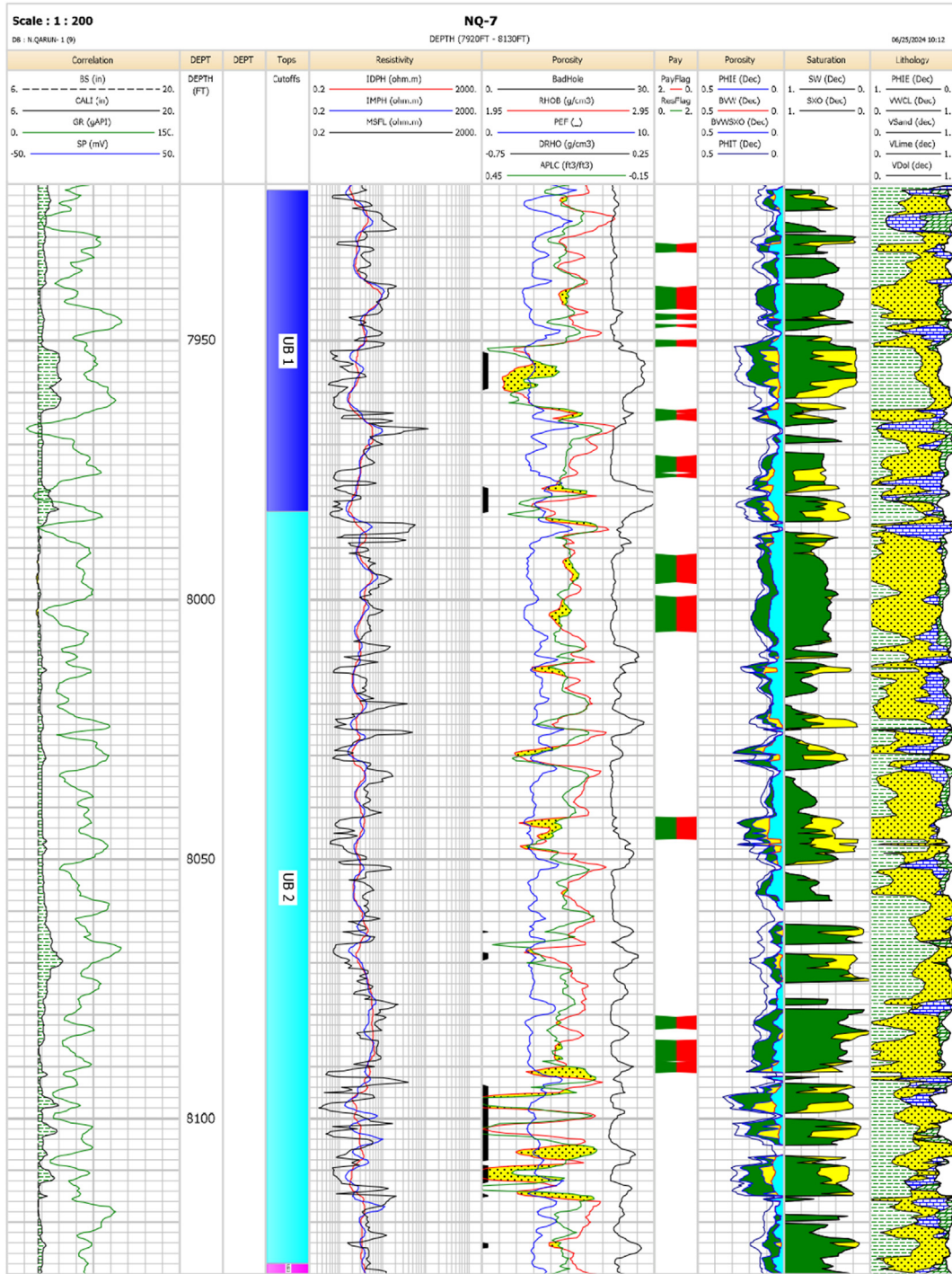


Fig. 12. Petrophysical evaluation for UB-1 and UB-2 zones in the NQ-7 well summarizes the pay results and depths.

upstructure and an increase toward the down-structure of the field. Specifically, the NQ-7 well shows the minimum volume of clay (9%), while the NQ-8 well shows the maximum volume of clay (13%) (Fig. 17).

#### 4.4.4. Water saturation distribution

The water saturation distribution map for the Upper Bahariya Formation (UB-1, UB-2) in the investigated wells of the North Qarun oil field shows very slight differentiation between water

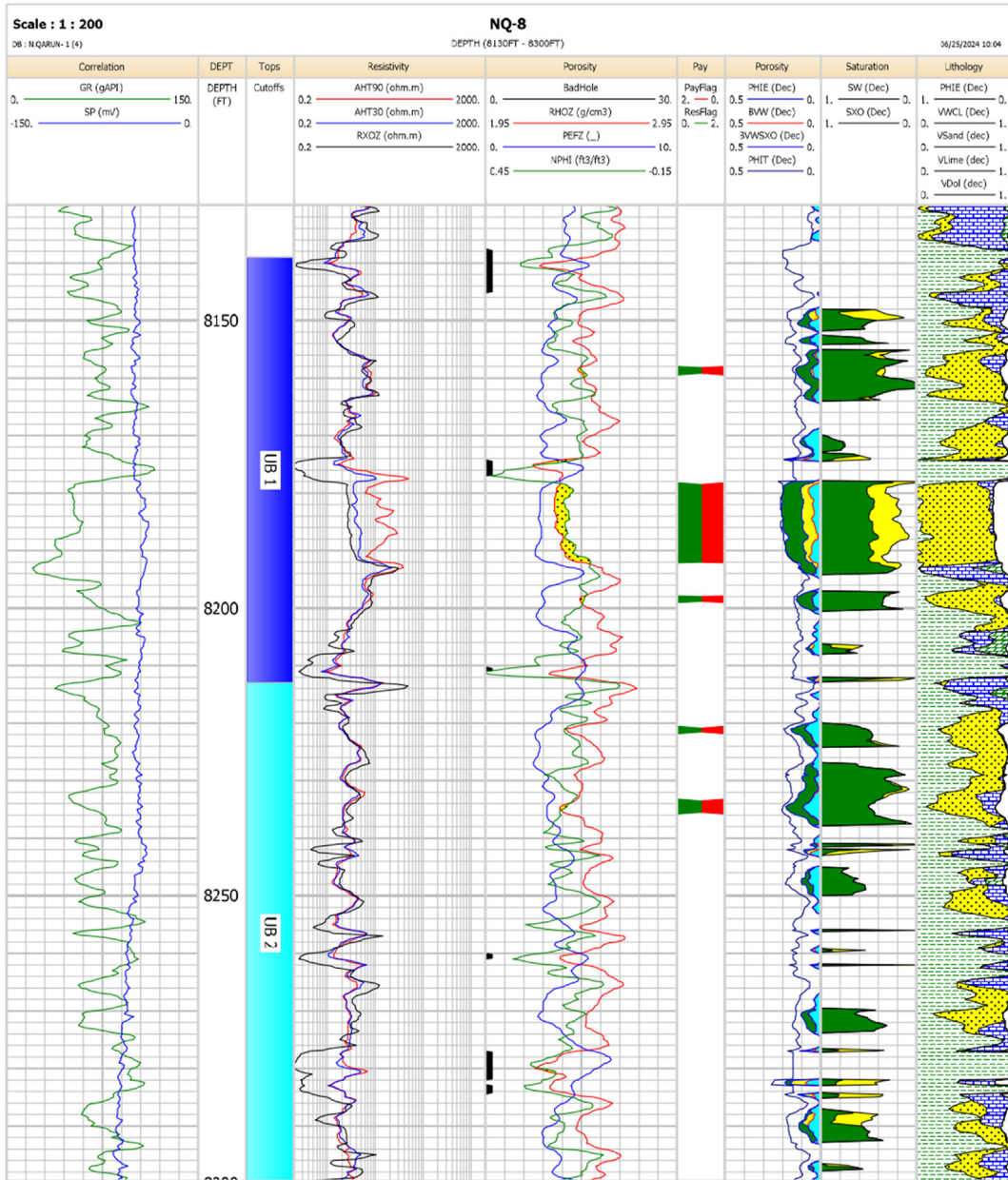


Fig. 13. Petrophysical evaluation for the UB-1 and UB-2 zones in the NQ-8 well summarizes the pay results and depths.

saturation values in the study area, with values ranging from 35 to 41% (Fig. 18).

4.5. Hydrocarbon volume calculation

Based on the provided information, it seems that preliminary hydrocarbon volumes have been estimated for the Upper Bahariya Formation (UB-1, UB-2) using a formula expressed in terms of stock tank of original oil in place (STOOIP). The formula used for estimation is: STOOIP (STB) = 7758 × A

× h × Φ<sub>eff</sub> × (1-S<sub>w</sub>) × N/G × 1/B<sub>0</sub>, where A is the reservoir area in acres, h the net pay thickness in feet, Φ<sub>eff</sub> the effective porosity in fraction, (1-S<sub>w</sub>) the hydrocarbon saturation in fraction, N/G the net to gross reservoir ratio, B<sub>0</sub> the formation volume factor, and 7758 is an acre foot conversion for oil.

The cumulative (STOOIP) estimated for zones is reported as 13.9 million stock tank barrels (MMSTB) as shown in Table 3.

This calculation method uses key reservoir input parameters derived from data obtained from the

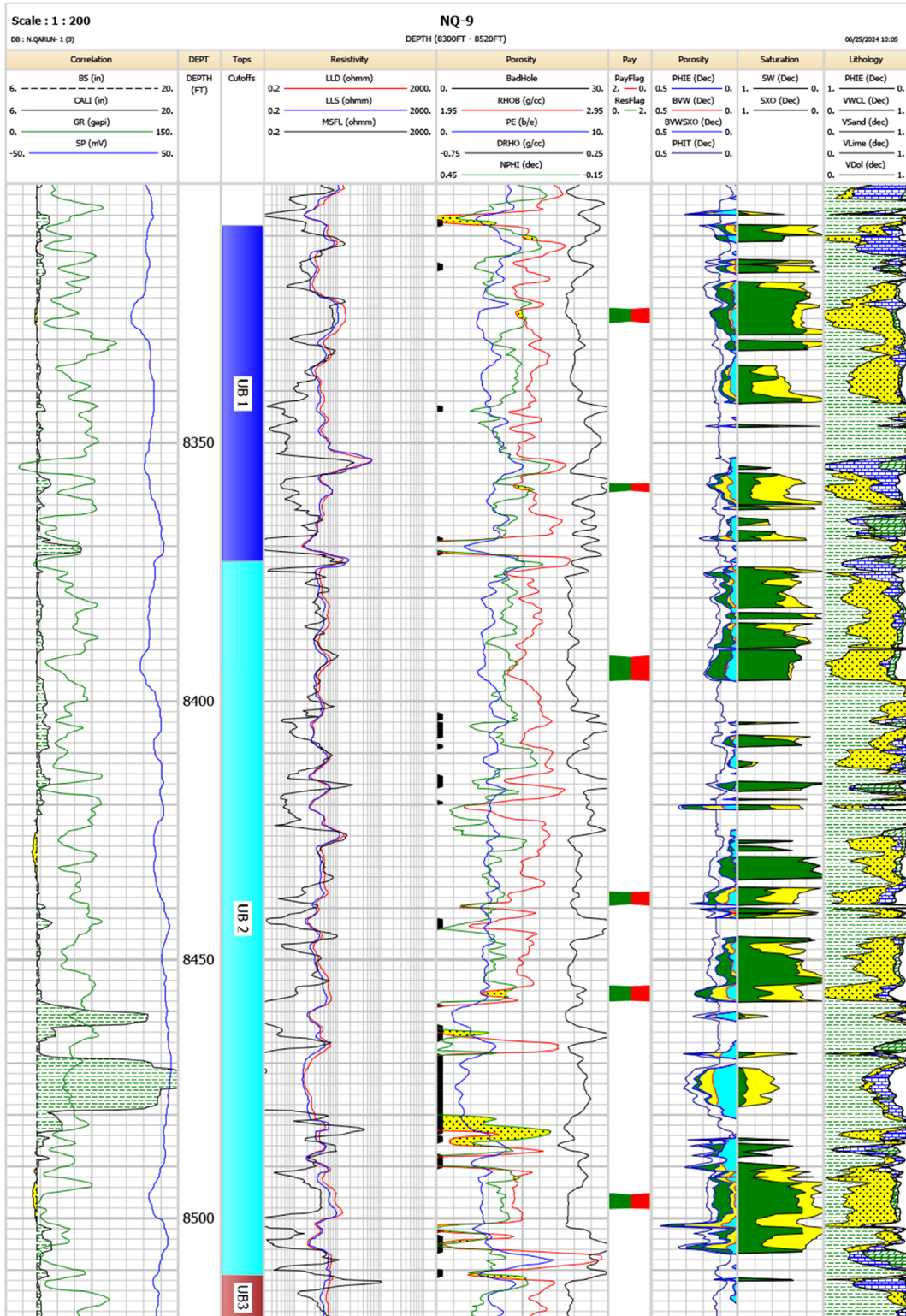


Fig. 14. Petrophysical evaluation for UB-1 and UB-2 zones in the NQ-9 well summarizes the pay results and depths.



Table 1. Total petrophysical summary table for Upper Bahariya Reservoir (UB-1, UB-2).

| Well name | Reservoir | Gross thickness (ft) | Net pay (ft) | Net/gross sand | EFF porosity % | Water saturation % | Shale volume % |
|-----------|-----------|----------------------|--------------|----------------|----------------|--------------------|----------------|
| N.QARUN-1 | UB-1      | 70                   | 22           | 31             | 20             | 41                 | 15             |
| N.QARUN-7 |           | 62                   | 9            | 14             | 15             | 42                 | 8              |
| N.QARUN-8 |           | 74                   | 16           | 22             | 18             | 24                 | 6              |
| N.QARUN-9 |           | 65                   | 4            | 6              | 15             | 44                 | 5              |
| N.QARUN-1 | UB-2      | 135                  | 15           | 11             | 24             | 35                 | 7              |
| N.QARUN-7 |           | 145                  | 27           | 19             | 17             | 38                 | 10             |
| N.QARUN-8 |           | 143                  | 4            | 3              | 16             | 48                 | 20             |
| N.QARUN-9 |           | 138                  | 13           | 9              | 17             | 38                 | 15             |

Table 2. Average petrophysical summary table for Upper Bahariya Reservoir (UB-1, UB-2).

| Well name | Reservoir | Gross thickness (ft) | Net pay (ft) | Net/gross sand | Average EFF porosity % | Average water saturation % | Average shale volume % |
|-----------|-----------|----------------------|--------------|----------------|------------------------|----------------------------|------------------------|
| N.QARUN-1 | UB        | 205                  | 37           | 42             | 22                     | 37                         | 11                     |
| N.QARUN-7 |           | 207                  | 36           | 33             | 16                     | 40                         | 9                      |
| N.QARUN-8 |           | 217                  | 20           | 25             | 17                     | 35                         | 13                     |
| N.QARUN-9 |           | 203                  | 17           | 15             | 16                     | 41                         | 10                     |

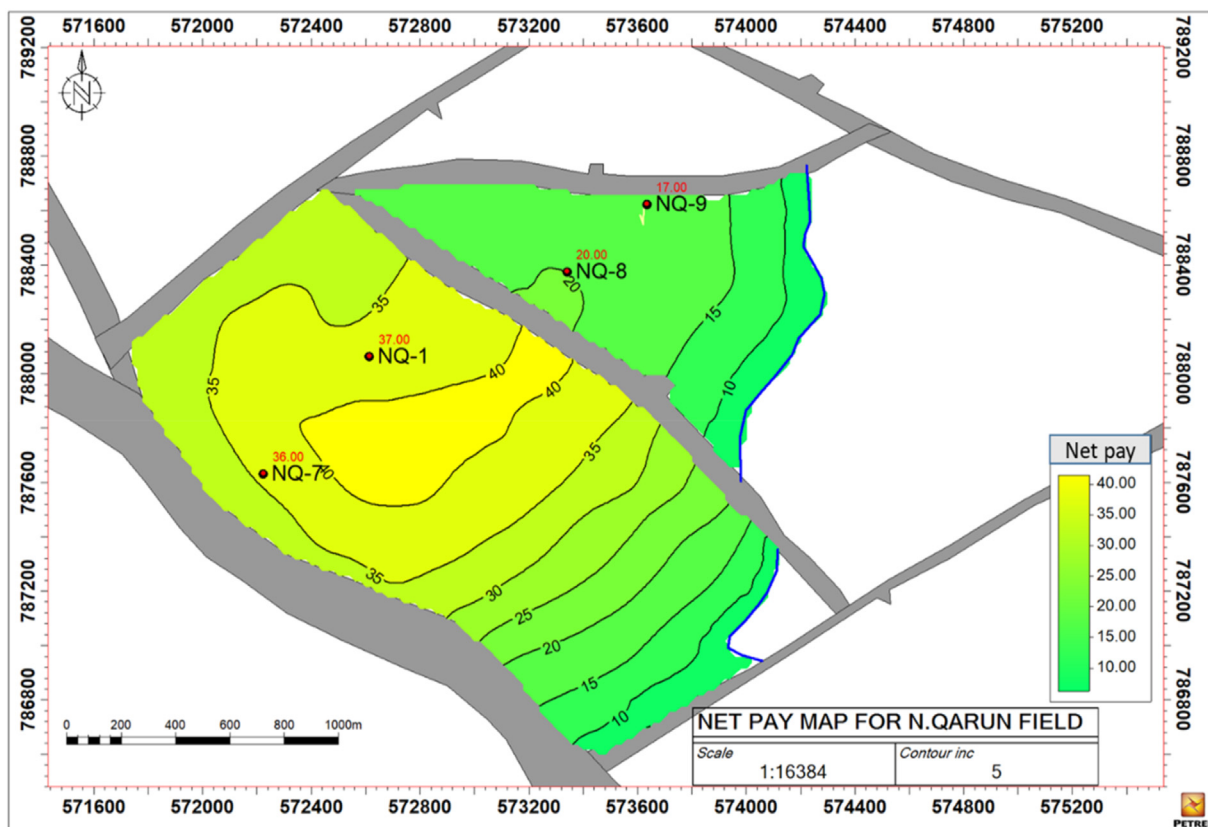


Fig. 15. Net pay thickness map for Upper Bahariya Formation (UB-1 and UB-2) shows increasing thickness toward the southwest part of the field.

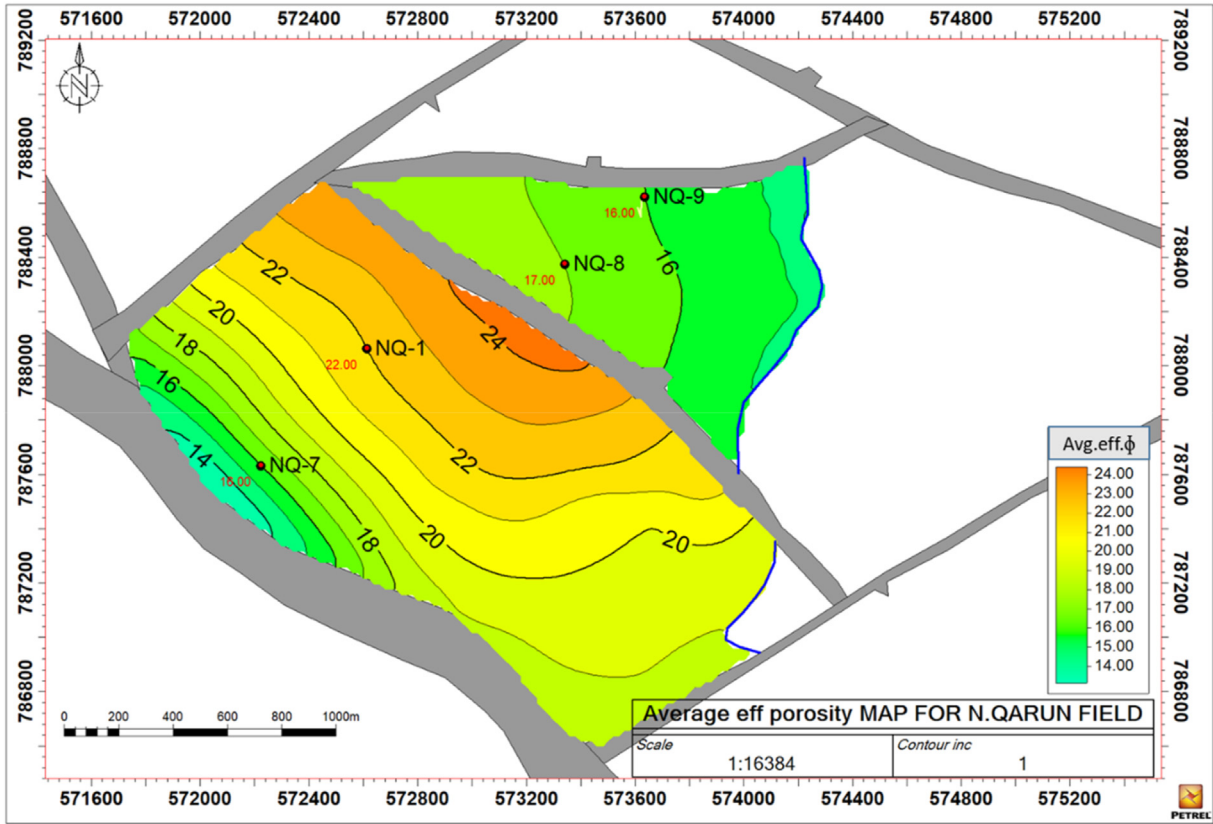


Fig. 16. Effective porosity map for Upper Bahariya Formation (UB-1, UB-2) shows an increase in the central part of the field.

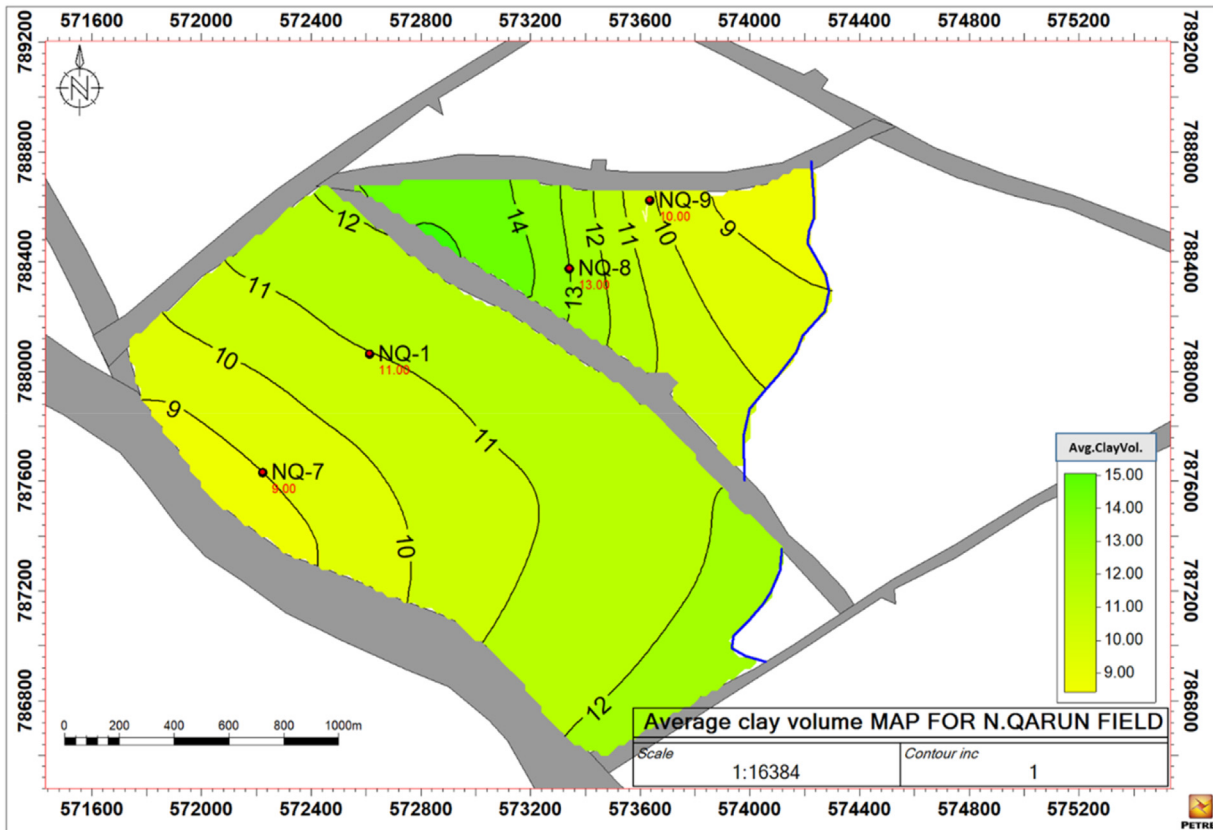


Fig. 17. Clay volume map for Upper Bahariya Formation (UB-1, UB-2) shows a decrease towards the upstructure.

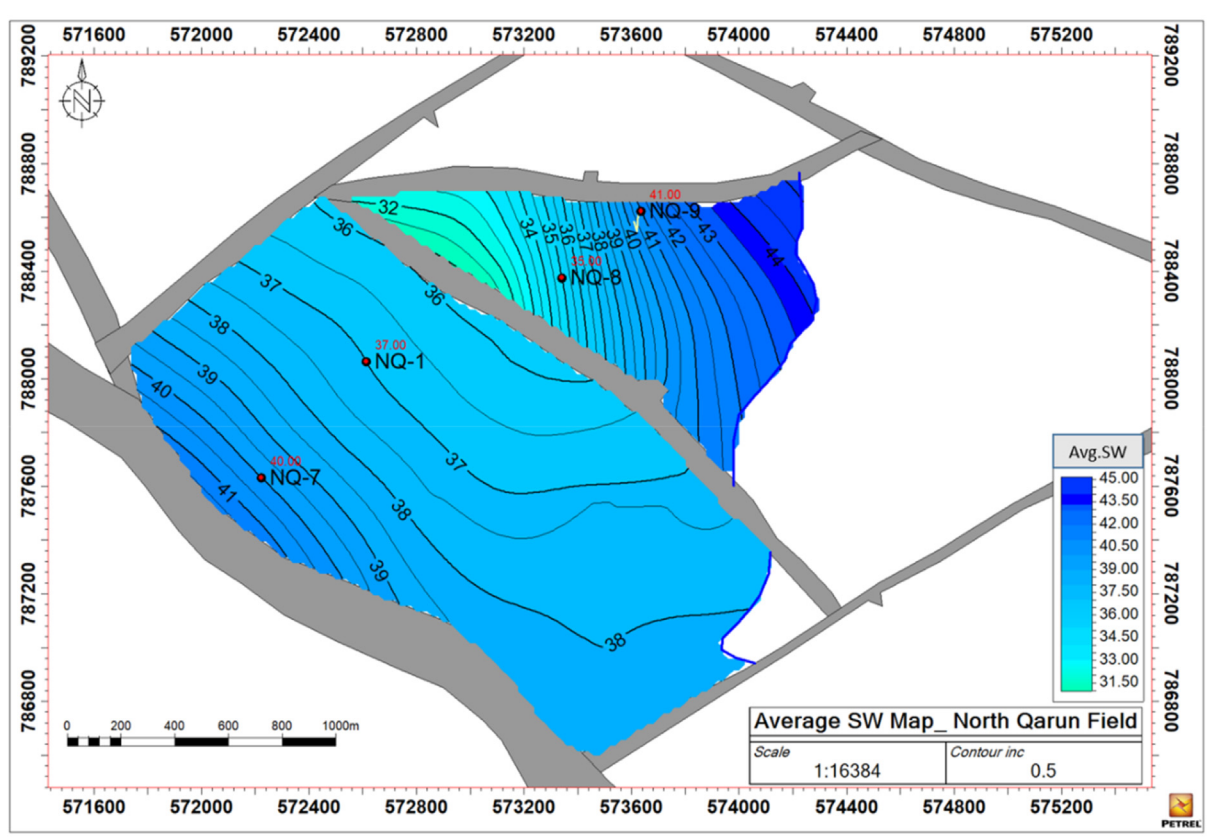


Fig. 18. Water saturation map for Upper Bahariya Formation (UB-1 and UB-2) shows very slight differentiation between water saturation values in the study area.

first four drilled wells penetrating the reservoir section. The estimated STOOIP provides an initial assessment of the potential hydrocarbon reserves within the Upper Bahariya Formation (UB-1, UB-2) based on the available geological data and reservoir characteristics.

#### 4.6. Conclusions

The geological findings elucidate the predominance of an echelon structures featuring double plunging anticlines bounded by NE reverse faults, intersected by NW normal faults, which experienced reactivation during the formation of the Gulf of Suez.

The petrophysical investigation aimed to discern productive strata, discriminates between hydrocarbon and aqueous phases within the reservoir, and delineate petrophysical parameters essential for subsequent modeling endeavors. Analysis unveiled lucrative reservoir intervals within the Upper Bahariya Formation (UB-1, UB-2).

By computing clay volume, water saturation, and average effective porosity, and implementing

Table 3. The stock tank original oil in place (STOOIP) estimated for the interested zones.

| Zone       | STOOIP MMSTB |
|------------|--------------|
| UB-1       | 5.02         |
| UB-2       | 8.88         |
| Cumulative | 13.9         |

cutoffs, the cumulative net pay values for the Upper Bahariya zones (UB-1, UB-2) were established for each borehole. Cartographic representation of petrophysical attributes of the Upper Bahariya Formation (UB-1, UB-2) reservoirs underscored the structural and facies-driven influences on net pay thickness, while effective porosity increases at the central part of the field, and the volume of clay decreases toward the upstructure and an increase toward the downstructure of the field. Minimal disparity in water saturation values was observed across the study area.

Based on the cumulative stock tank of original oil in place (STOOIP) estimated for zones is 13.9 million stock tank barrel of oil.

## Authors contributions

Ahmed Soliman Ahmed: writing, Software, editing, methodology, formal analysis. Tharwat Helmy Abdel Hafeez: review & editing, visualization, supervision. Mohamed Mosaad Mohamed: Original draft, resources, data curation.

## Funding

No funding.

## Ethics information

There is no conflicts of interest.

## Conflicts of interest

There are no conflicts of interest.

## Acknowledgments

The authors express their gratitude to the Egyptian Petroleum Corporation (EGPC) and Khalda Petroleum Company (KPC) and to the staff at Al-Azhar University. Data Approved by “EGPC” Egyptian General Petroleum Corporation and khalda Petroleum Company.

## References

- [1] Abu El Naga M. In Paleozoic and Mesozoic depocenters and hydrocarbon generating areas, Northern Western Desert. In: Proc 7th Egypt Gen Petrol Corporat Explorat Prod Conf Cairo. 8; 1984. p. 269–87.
- [2] Abd El-Aziz Mohamed. Tectonic Evolution of the Kattaniya High and El-Gindi Basin (Western Desert, Egypt) and Their Hydrocarbon Potentialities. PhD Thesis 2001. Cairo, Egypt: Ain Shams University; 2001. p. 180.
- [3] Said R. Cretaceous paleogeographic maps. Geol Egypt 2017: 439–49. Published on 25 October 2017.
- [4] Moustafa AR. Wrench tectonics in the north Western Desert of Egypt (Abu Roash area, southwest of Cairo). Middle East Res Center Ain Shams Univ Earth Sci Series 1988;2:1–6.
- [5] Schlumberger, Well Evaluation Conference, Egypt. Chester: Schlumberger technical editing services; 1995. p. 57–68.
- [6] Meshref WM. Tectonic framework. Geol Egypt 2017:113–55. <https://doi.org/10.1201/9780203736678>. Published on 25 October 2017.
- [7] Said R. Tectonic framework of Egypt. In: In the Geology of Egypt. Amsterdam: Elsevier Publishing Company; 1962. p. 28–44.
- [8] Bayoumi T. The influence of interaction of depositional environment and syndepositional tectonics on the development of some Late Cretaceous source rocks, Abu Gharadig Basin, Western Desert, Egypt. In: 13th Egyptian General Petroleum Corporation Exploration and Production Conference, Cairo, Egypt. 2; 1996. p. 475–96.
- [9] Abd El-Aziz M, Moustafa AR, Said SE. Impact of basin inversion on hydrocarbon habitat in the Qarun Concession, Western Desert, Egypt. In: Proceedings of 14th Egyptian General Petroleum Corporation Exploration and Production Conference, Cairo. 1; 1998. p. 139–55.
- [10] Moustafa AR. Mesozoic-Cenozoic basin evolution in the northern Western Desert of Egypt. In: 3rd Symposium on the Sedimentary Basins of Libya, the Geology of East Libya. 3; 2008. p. 29–46.
- [11] Schlumberger, Log Interpretation Charts Book. Texas 77478: Sugar Land; 2009. p. 238.